Beyond Element-Specific Magnetism: Resolving Inequivalent Nd Crystal Sites in $Nd_2Fe_{14}B$

Daniel Haskel, Jonathan Lang, Zahirul Islam, George Srajer, Julie Cross, and Paul Canfield

***Abstract*—We show how basic crystallography can be combined with resonant scattering of circularly polarized (CP) X-rays to extract element- and site-specific magnetism in crystals. This is achieved by combining the inherent element specificity of resonance scattering with the symmetry properties of the crystal, which results in enhanced/suppressed scattering amplitudes from certain lattice sites under particular diffraction conditions. We used this method to measure the magnetic response of inequivalent Nd sites in $Nd_2Fe_{14}B$ single crystal ($4f$ and $4g$ sites in Wyckoff notation) through the crystal's magnetization reversal at room temperature and through the spin reorientation transition at lower temperatures. This approach might prove very valuable in studies of magnetocrystalline anisotropy in complex materials with multiple elements and crystal sites.**

***Index Terms*—Anisotropy, anomalous scattering, circular polarization, crystal fields, inequivalent crystal sites, magnetic circular dichroism, resonant magnetic scattering, XMCD.**

I. Introduction

THE ability of X-ray based techniques to separate magnetic contributions from different elements in a sample (element-specificity) has proven to be very valuable in studies of complex magnetic materials. In the case of X-ray magnetic circular dichroism (XMCD), this separation is achieved by tuning the x-ray energy to element-specific electron excitations whose response to circularly polarized (CP) X-rays of opposite helicities can be used to extract magnetic information from the excited element only [1], [2].

The complexity of magnetic materials, however, goes beyond the presence of multiple chemical species: many materials feature elements of the same specie in inequivalent crystal sites. These crystal sites are dictated by the symmetry group of the crystal (space group) with atoms in different crystal sites residing in unique crystalline environments. Currently used X-ray based techniques, such as XMCD, average over these inequivalent crystal sites. However, retrieving magnetic information from these sites is of paramount importance, for example, in understanding the atomic origins of magnetocrystalline anisotropy (MCA), which is strongly tied to the local crystalline environment through crystal field effects. In the case of $Nd_2Fe_{14}B$, it is generally agreed that Nd magnetic moments dominate the MCA (over Fe moments) due to the large orbital magnetic moment associated with their $4f$ electrons [3]. In this structure, however, there exists two Nd inequivalent sites ($4f$ and $4g$ in Wyckoff notation) in quite distinct atomic environments. Spin-dependent density functional theoretical calculations (LSDA) show that the crystal field at the Nd inequivalent crystal sites is markedly different [4]–[7], leading to the expectation that their intrinsic MCA will differ as well. While this has broad implications, not only for understanding the atomic origin of MCA in this material but for the mechanism of the spin-reorientation transition from c axis toward the basal plane at $T \approx 130$ K, the magnetic responses of these inequivalent sites could not as yet be separated.

Manuscript received October 15, 2003. The work performed at Argonne National Laboratory was supported by the U.S. Department of Energy, Office of Science, under Contract W-31-109-ENG-38.

D. Haskel, J. Lang, Z. Islam, and G. Srajer are with the Advanced Photon Source, Argonne National Laboratory, Argonne, IL 60439 USA (e-mail: haskel@aps.anl.gov).

J. Cross is with the Pacific Northwest Consortium, University of Washington, Seattle, WA 98195 USA.

P. Canfield is with the Department of Physics and Ames Laboratory, Iowa State University, Ames, IA 50011 USA.

Digital Object Identifier 10.1109/TMAG.2004.832675

II. Fundamental Principles

In magnetic materials the resonant (anomalous) scattering of circularly polarized X-rays is modified from the scattering that occurs in nonmagnetic materials. This is because the virtual photoelectron that is excited from the core state to the intermediate, resonance state, is partially spin-polarized and therefore becomes sensitive to the spin imbalance in the density of states near the Fermi level. The electric dipole scattering amplitude from a single magnetic ion near resonance is then given by [8]

$$f = f_e(\mathbf{Q}, E)(\hat{\boldsymbol{\epsilon}}' \cdot \hat{\boldsymbol{\epsilon}}) - i f_m(E)(\hat{\boldsymbol{\epsilon}}' \times \hat{\boldsymbol{\epsilon}}) \cdot \hat{\mathbf{m}} \qquad (1)$$

where we neglected the much smaller linear dichroism and nonresonant magnetic scattering terms. The term f_e includes nonresonant (Thomson) and resonant charge scattering while f_m is purely resonant magnetic scattering, $(\hat{\epsilon}, \hat{\epsilon}')$ are incident and scattered polarization vectors, and $\hat{\mathbf{m}}$ is magnetic moment direction. Both f_e and f_m are complex and strongly energy dependent, their imaginary parts being responsible for X-ray absorption and magnetic circular dichroism, respectively. The scattered intensity $I(\mathbf{Q}, E)$ from a crystal of magnetic ions is then given by the modulus square of the structure factor, $F(\mathbf{Q}, E) = \sum_i (A f_e - iBf_m) e^{i\mathbf{Q}\cdot\mathbf{r}_i}$, with $A = (\hat{\boldsymbol{\epsilon}}' \cdot \hat{\epsilon})$ and $B = (\hat{\boldsymbol{\epsilon}}' \times \hat{\boldsymbol{\epsilon}}) \cdot \hat{\mathbf{m}}$. The sum is over all atoms in the unit cell and thermal disorder in atomic positions is neglected

$$I(\mathbf{Q}, E) = \sum_{i,j} (A f_e - iBf_m)_i^* (A f_e - iBf_m)_j e^{i\mathbf{Q}\cdot(\mathbf{r}_i - \mathbf{r}_j)}. \qquad (2)$$

The scattered intensity of (2) contains pure charge terms ($A^2 f_{e,i}^* f_{e,j}$, independent of $\hat{\mathbf{m}}$), pure magnetic terms ($B^2 f_{m,i}^* f_{m,j}$, proportional to $\hat{\mathbf{m}}^2$) and charge-magnetic interference terms of the form $A^* B f_{e,i}^* f_{m,j}$, proportional to

TABLE I
SITE-SPECIFIC Nd STRUCTURE FACTORS, $F_{\mathbf{Q}} = f_{\mathrm{Nd}} \sum_{i=1}^{4} e^{i\mathbf{Q}\cdot\mathbf{r}_i}$, FOR A FEW BRAGG REFLECTIONS WITH SCATTERING VECTORS ALONG THE [110] DIRECTION. RESONANT CHARGE CONTRIBUTIONS TO f_{Nd} AT Nd L_2 RESONANCE ARE FROM TABULATED VALUES. $\mathbf{Q} = 2\pi(h/a, k/b, l/c); \mathbf{r}_i = (x_i a, y_i b, z_i c)$. STRUCTURAL PARAMETERS ARE FROM HERBST [3]

Wyckoff Site	(110)	(220)	(440)
4f	2.2 + 0.5i	140 + 35i	86 + 29i
4g	69 + 15i	5.2 + 1.3i	92 + 31i

$\hat{\mathbf{m}}$. Since reversing X-ray helicity is equivalent to reversing the magnetization direction, by measuring the *difference* in scattering intensity between opposite helicities of CP X-rays, $(I^+ - I^-)$, the pure charge and magnetic scattering terms vanish and only the charge-magnetic interference terms contributes. This differential measurement results in a scattered intensity that (a) is proportional to the magnitude of the magnetic moment, through f_m, and contains information about the moment's direction relative to the X-ray polarization vectors, through $(\hat{\epsilon}' \times \hat{\epsilon}) \cdot \hat{\mathbf{m}}$. The differential measurement provides a mechanism to remove the strong pure charge scattering term, which for rare-earth L-edges, is $\approx$100 times stronger than the charge-magnetic interference term. This is particularly important in ferro(ferri)-magnets, where the chemical and magnetic periodicities are the same resulting in overlapping charge and magnetic Bragg peaks in reciprocal space. Since $f_m \ll f_e$ the resonant charge scattering is obtained from $(I^+ + I^-)$. We define the flipping ratio as the charge-normalized difference signal, $(I^+ - I^-)/(I^+ + I^-)$.

With no polarization analysis performed on the scattered beam the angular dependence of the charge-magnetic interference scattering was calculated for our geometry using the density matrix formalism of Blume and Gibbs[9], [10]. This involves representing A and B of (2) in the (σ, π) matrix representation and taking traces over matrix products of the form $[\hat{\epsilon}' \cdot \hat{\epsilon}]^* \rho [(\hat{\epsilon}' \times \hat{\epsilon}) \cdot \hat{m}]$, where ρ is the density matrix of a circularly polarized incident beam. The resultant angular dependence is given by $[(\hat{k}_i \cdot \hat{m}) \cos 2\theta + (\hat{k}' \cdot \hat{m})]$, where $(\hat{k}, \hat{k}')$ are incident and scattered wave vectors, respectively. It follows that the charge-magnetic interference *difference* scattering signal is only sensitive to the magnetization component in the scattering plane.

Site selectivity is achieved by exploiting the symmetry properties of the crystal. Neodymium–iron–boron ($Nd_2Fe_{14}B$) has a $P4_2/mnm$ tetragonal space group with four formula units per unit cell. The 56 Fe atoms are distributed among six inequivalent crystal sites, while the 8 Nd atoms occupy two other inequivalent sites $(4f, 4g)$. As shown in Table I, by selecting scattering vectors along the high-symmetry [110] direction, structure factor contributions from either one or the other Nd sites nearly vanish. For example, diffraction from (110) planes probes the Nd at $4g$ sites; diffraction from (220) planes probes the Nd at $4f$ sites; and nearly equal contributions are measured for a (440) reflection. We note that charge-magnetic interference scattering at these $\mathbf{Q}$ vectors includes charge-scattering contributions from Fe and B atoms as well. However, since the experiments are performed near the Nd L_2 resonance, the scattered intensity contains magnetic contributions from only Nd sites (f_m is practically zero away from resonance).

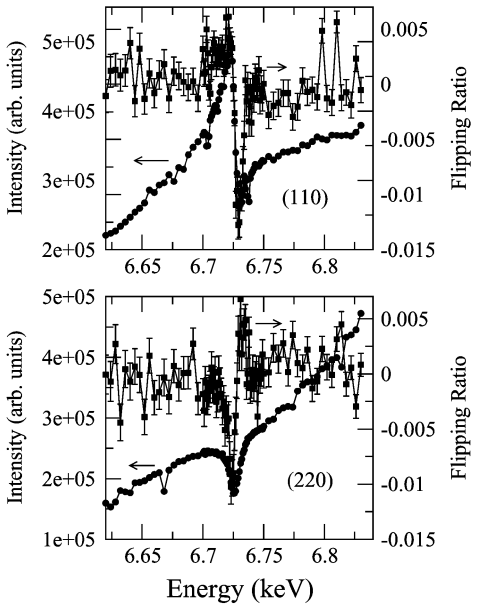

Fig. 1. Resonant charge (circles) and charge-magnetic interference (squares) scattered intensities obtained by adding and subtracting scattered intensities for opposite, incident X-ray helicities. The X-ray helicity is switched at each energy point, and the diffraction condition is maintained at each energy. Measurements were done at $T = 300$ K with an $H = 6$ kOe magnetic field applied along the [001] direction, which is contained in the scattering plane.

III. EXPERIMENTAL RESULTS

The X-ray measurements were performed at undulator beamline 4-ID-D of the Advanced Photon Source. Undulator radiation was monochromatized with a Si (111) double-crystal monochromator and its polarization converted from linear to circular with a diamond (111) phase retarder operated in Bragg transmission geometry. A ($\approx$5 × 3 × 2 mm^3) single crystal was placed in the field of an electromagnet ($\pm$6 kOe) for room-temperature measurements or a permanent magnet (2.4 kOe) for low-temperature measurements. The crystal was aligned with its [110] facet oriented along the scattering vector and the magnetic field applied along the [001] direction, which was parallel to the sample surface and in the scattering plane. A closed-cycle He refrigerator mounted in the ϕ circle of a diffractometer was used for the low-temperature measurements. The resonant diffraction measurements were carried out through the Nd L_2 resonance ($2p_{1/2}$ excitation at 6.722 keV) by switching the helicity of the incident CP X-rays at each energy point while maintaining a given diffraction condition (fix $\mathbf{Q}$) at all energies. X-ray magnetic circular dichroism measurements were simultaneously performed by measuring the difference in Nd L_β fluorescence intensity for opposite X-ray helicities at each energy point through the Nd L_2 absorption edge using energy-dispersive Ge solid-state detectors.

Fig. 1 shows resonant diffraction data through the Nd L_2 edge under (110) and (220) diffraction conditions. As seen in Table I, these reflections alternately probe $4g$ and $4f$ sites, respectively. Element- and site-specific hysteresis loops (Fig. 2) were performed under these diffraction conditions by recording changes

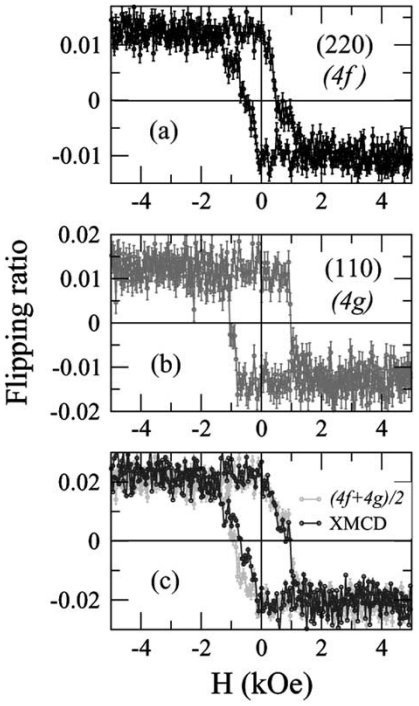

Fig. 2. Element- and site-specific hysteresis loops at $T = 300$ K. The magnetic field is applied along the [001] easy-axis direction. (a) (220) Bragg reflection, $E = 6.724$ keV; (b) (110) Bragg reflection, $E = 6.730$ keV; and (c) comparison of the average of site-specific signals from scattering channel with the result obtained in the absorption (XMCD) channel. The latter measures a weighted average of the two sites. Signals in (c) are scaled to match in the y axis.

in the flipping ratio as an applied field was looped while maintaining the diffraction condition at a fixed energy that optimizes the magnetic contrast. The response of the magnetic moment at each of the Nd inequivalent sites to the spin-reorientation transition (SRT) is obtained by measuring the T-dependent flipping ratio for the different diffraction conditions. Since $Nd_2Fe_{14}B$ is a high- temperature ferromagnet ($T_c \sim 585$ K), the magnitude of the Nd moments is practically constant below room temperature. Changes in measured intensities are due to the angular dependence of the charge-magnetic interference scattering as the magnetization reorients from a [001] easy-axis toward the basal plane. The angular dependence given above was used to extract the rotation of the Nd moments at each site through the SRT, shown in Fig. 3.

IV. Discussion

Fig. 2 clearly shows a different response of magnetic moments at inequivalent Nd sites to a looping applied field along the easy c axis. The $4g$ site requires a larger field and reverses more sharply compared to the $4f$ site. This originates in their distinct crystalline environments yielding different magnetocrystalline anisotropy constants. In fact, significant differences in crystal electric field parameters acting on the two Nd sites have been reported in some theoretical treatments [4]–[7]. It has also been suggested that a competition between the anisotropies at the two Nd sites is responsible for the

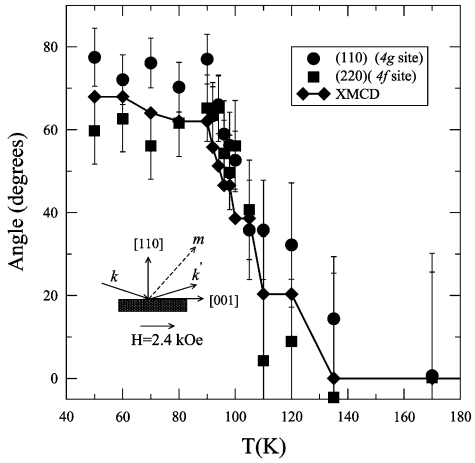

Fig. 3. Site-specific spin reorientation transition for inequivalent Nd sites. The angle between the component of the Nd magnetic moment in the scattering plane and the [001] crystallographic axis is separately shown for each site. Data points are integrated intensities of charge-magnetic interference scattering at each reflection. The average angular deviation obtained from the simultaneous absorption measurement is also shown.

SRT at $T \approx 130$ K [7]. Fig. 3 shows that the total angular deviation of magnetic moments from the c axis differs for the inequivalent Nd sites. The deviation from collinearity between the two Nd sublattices reaches $\approx 15^\circ$ at 50 K. The site-averaged angular deviation obtained from XMCD measurements is also shown in Fig. 3 and is in reasonable agreement with previous measurements [11]. The data may also indicate that the $4g$ sites drive the SRT, as those moments start reorienting at a higher temperature than those at $4f$ sites.

Acknowledgment

The authors would like to thank A. Cady and M. Newville for helpful discussions.

References

[1] G. Schütz *et al.*, "Absorption of circularly polarized x-rays in iron," *Phys. Rev. Lett.*, vol. 58, p. 737, 1987.
[2] J. Stöhr, "Principles of x-ray magnetic dichroism spectromicroscopy," *Surf. Rev. Lett.*, vol. 5, p. 1297, 1998.
[3] J. F. Herbst, "$R_2Fe_{14}B$ materials: Intrinsic properties and technological aspects," *Rev. Mod. Phys.*, vol. 63, p. 819, 1991.
[4] D. Sellmyer *et al.*, "Electronic structure and magnetism of $Nd_2Fe_{14}B$ and related compounds," *Phys. Rev. Lett.*, vol. 60, p. 2077, 1988.
[5] S. Jaswal, "Electronic structure and magnetism of $R_2Fe_{14}B$ (R = Y, Nd) compounds," *Phys. Rev. B*, vol. 41, p. 9697, 1990.
[6] K. Hummler and M. Fähnle, "Ab initio calculations of local magnetic moments and the crystal field in $R_2Fe_{14}B$ (R = Gd, Tb, Dy, Ho and Er)," *Phys. Rev. B*, vol. 45, p. 3161, 1992.
[7] D. Givord *et al.*, "Magnetic properties of $Y_2Fe_{14}B$ and $Nd_2Fe_{14}B$ single crystals," *Solid State Commun.*, vol. 51, p. 857, 1984.
[8] J. P. Hannon *et al.*, "X-ray resonance exchange scattering," *Phys. Rev. Lett.*, vol. 61, p. 1245, 1988.
[9] M. Blume and D. Gibbs, "Polarization dependence of magnetic x-ray scattering," *Phys. Rev. B*, vol. 37, p. 1779, 1988.
[10] J. P. Hill and D. F. McMorrow, "X-ray resonant exchange scattering: Polarization dependence and correlation functions," *Acta Cryst.*, vol. A52, p. 236, 1996.
[11] J. Chaboy *et al.*, "X-ray magnetic circular dichroism probe of a non-collinear magnetic arrangement below the spin reorientation transition in $Nd_2Fe_{14}B$," *Phys. Rev. B*, vol. 57, p. 8424, 1998.